

Entangled Polymers: Constraint Release, Mean Paths, and Tube Bending Energy

D. J. Read,^{*,†} K. Jagannathan,[†] and A. E. Likhtman^{*}

Department of Applied Mathematics, University of Leeds, Leeds, LS2 9JT, U.K., and
Department of Mathematics, University of Reading, Reading RG6 6AX, U.K.

Received May 1, 2008; Revised Manuscript Received July 8, 2008

ABSTRACT: Constitutive equations for entangled polymer melts and solutions are often derived from single chain tube models. Instead of keeping the chain coordinates, these models operate with a coarse-grained description in terms of positions of the tube segments. The dynamics of the tube is then imposed by constraint release, tube renewal at the ends, and deformation by the flow. However, the step of coarse-graining is rarely discussed, and the tube free energy and tube statistics are not derived. Moreover, the microscopic definition of the tube is rarely specified. In this paper we propose to define the tube as a mean path, i.e., a line connecting positions of each monomer averaged over entanglement relaxation time τ_e . We propose one simple model where such a coarse-graining step can be performed exactly, resulting in a free energy containing the usual Gaussian chain term and an additional bending energy term. This free energy leads to a path in space which is locally smooth and differentiable but has random walk statistics at length scales larger than the tube diameter. This eliminates several problems in previous tube models which use derivatives over contour variables. We then proceed to modify the constitutive equation of Graham et al. (2003) to include the bending energy in constraint release terms. The resulting theory does not contain uncertainties of the original theory and has a clearer and better defined microscopic origin.

1. Introduction

Recent research into the rheological properties of entangled polymeric liquids has focused on the dynamics of the polymer chains under flow.¹ Entanglements—the constraints imposed on the dynamics of a given chain by virtue of the fact that it cannot cross surrounding chains—are commonly described either by invoking the concept of a “tube” surrounding the chain (as in the tube constitutive model of Doi and Edwards,² from which most current theoretical modeling is derived) or in terms of “sliplinks”,^{3–6} which generally lead to solution via stochastic simulation.

An important dynamical process in either description of entangled polymers is that of “convective constraint release” (CCR), proposed by Marucci⁷ to resolve discrepancies between experiment and the model of Doi and Edwards² in the fast flow regime. Contrary to most experimental observations (but note some recent experiments, for example ref 8) the Doi–Edwards model predicts a maximum in the steady state shear stress as a function of strain rate in simple shear flows. This occurs because shear flow rotates and aligns entanglement tubes into the velocity direction of the flow, so there is no component of the entropic chain force in a suitable direction to give a shear stress. The CCR mechanism invokes the fact that, when a chain end passes through a particular region of the polymer, it releases any contribution to the entanglement constraints provided by that chain on the surrounding polymers in the local region. Chain retraction occurring in the nonlinear flow regime pulls chain ends through the entanglement mesh, thus producing constraint release events. In extremely fast flows, greater than the inverse of the stretch time τ_R of the polymer, chains stretch in the tube, so that both CCR and chain stretch are important for the rheological modeling of polymer melts and solutions.

A number of theories have been proposed to include the effects of CCR and stretch into a constitutive framework using

the tube model.^{9–13} The work reported in this present paper aims in part to investigate issues raised in the papers of Graham et al.¹² and subsequently Read.¹³ These two papers both recognize that constraint release produces local hops of the tube and that the Rouse model describes the generic dynamics for a connected random walk undergoing local hops. Consequently, they treat constraint release by modeling the tube using a modified Rouse model. However, it appears (according to Read)¹³ that the results of these models (for example, in terms of the stress during start-up of steady shear) are highly sensitive to the assumed form of the tube hops, especially in the chain stretching limit. This sensitivity was such that, depending upon the choice of seemingly arbitrary parameters, *qualitatively* different constitutive behavior could be obtained, so fits to data required a judicious choice of parameters but without obvious physical justification.

The deep reason for this model arbitrariness is that in all constraint release papers the underlying microscopic tube picture is not specified. Consequently, the model for constraints and thus constraint release is formulated in an ad hoc fashion. The main goal of this paper is to propose a microscopic definition of the tube and constraint release events, which removes this apparent oversensitivity to the choice of parameters and arbitrariness in their choice. It is also our hope that the concepts introduced will prove useful in future investigations into the tube model and its relation to other models and simulation schemes.

2. Constraint Release in Previous Models

Before introducing our model, we shall briefly review some previous approaches to the tube modeling. The papers of Graham et al.¹² and Read¹³ share a common description of the constraint release process. The form of the constraint release equations were obtained by Graham et al. by considering random hops of a set of connected “beads” representing the tube path. This gives rise to an equation of motion for the position, $\mathbf{R}(s)$, of the tube (where the variable s is used to count units of entanglement degree of polymerization N_e along the enclosed

* To whom correspondence should be addressed.

[†] University of Leeds.

^{*} University of Reading.

chain). This, when written in discrete coordinates, is similar to the Rouse model:

$$\frac{\partial \mathbf{R}(s)}{\partial t} = \cdots + \frac{3\nu}{2}(\mathbf{R}(s+1) + \mathbf{R}(s-1) - 2\mathbf{R}(s)) + \mathbf{g}(s, t) \quad (1)$$

where the constraint release rate ν is self-consistently determined in the model solution. In this discrete model, the random noise $\mathbf{g}(s, t)$ has statistics such that

$$\langle g_\alpha(s, t) g_\beta(s', t') \rangle = \nu a^2 \delta_{s,s'} \delta(t-t') \delta_{\alpha\beta} \quad (2)$$

As they stand, these two equations are not easily combined with a description of reptation or chain retraction (which require a smooth, differentiable, space curve $\mathbf{R}(s)$ with continuous coordinate s —they require that the tube path exists in between the beads). There is also ambiguity as the chain stretches, since it is not clear whether one should keep a constant number of beads (Z , one per original tube diameter) or increase the number of beads as the length of the tube increases. These two problems are both concerned with the tube properties at length scales of order the tube diameter or lower. The above equations—and equations derived from them—adequately describe the dynamics at larger length scales than the tube diameter, but they contain no information about smaller length scales. To proceed further appears to require further assumptions.

Graham et al. and, following them, Read both make the transformation to continuous coordinates by replacing the discrete difference in (1) with a continuous derivative

$$\mathbf{R}(s+1) + \mathbf{R}(s-1) - 2\mathbf{R}(s) \rightarrow \mathbf{R}''(s)$$

and then by replacing the Kronecker delta in (2) with a function of finite width in the continuous s coordinate

$$\delta_{s,s'} \rightarrow \Delta(s-s')$$

The resulting equations do describe a smooth space curve $\mathbf{R}(s)$, but one in which the smoothness at equilibrium is set by the width of the noise function $\Delta(s-s')$. At this point, one can detect a possible problem, since (i) the smoothness at equilibrium should be set by a free energy, not the stochastic noise, and (ii) for a finite width noise, there should (by the fluctuation–dissipation theorem) be a corresponding finite width in the dissipative term of the equations (as in, for example, eqs 19 and 20 derived below).

To incorporate chain stretch, Graham et al. (i) keep the number of beads fixed in the sense that the noise width $\Delta(s-s')$ remains fixed but (ii) renormalize the effective hop rate to account for both an increased chain tension along the tube and an increased number of tube segments along the stretched chain. The result is an extra factor of λ^{-1} (where $\lambda = |\mathbf{R}'(s)|/a$ is the chain stretch) in the dissipative term of eq 1 and in the noise amplitude of eq 2. This is one of several possible assumptions which give the same large-scale dynamics, but possibly different small-scale dynamics. Read explored other possible assumptions (e.g., increasing the effective number of beads with chain stretch) and found that a wide range of results could be obtained in start-up shear.

As indicated in the Introduction, the main goal of this paper is to rectify these ambiguities by obtaining a description of the tube, and of constraint release hops, which is valid at the length scale of the tube diameter and below. In particular, we shall seek a description in which the equilibrium tube path is not set by stochastic noise but by a free energy, suitably derived.

3. Mean Path in the Warner–Edwards Model

It is worth giving brief consideration toward what is actually meant by “the tube” in theories of entangled polymer dynamics. The concept is this: it is a path in space such that the enclosed

chain is constrained to fluctuate around this path by a distance of order the tube diameter (although motion along the tube path is permitted). At length scales larger than the tube diameter, it is a coarse-grained random walk (as it must be, given that it encloses the chain, which is itself a random walk). The fathers of the tube theory were quite careful about this point. In particular, de Gennes¹⁴ explicitly commented that statistics and the structure factor of the tube on the length scale of tube diameter require additional assumptions which are not specified. The later tube theories of Graham et al.¹² seem to require that it is smooth and differentiable at smaller length scales. Otherwise, the tube tangent (used in the calculation of the stress) is not defined, nor is the tube length (used in the calculation of the reptation, or escape, time). Here, we seek a description that retains these features, but which holds the possibility of comparison with more detailed models of entangled chain dynamics (such as the slip-tube model³ or molecular simulation¹⁵).

The idea that the chain “fluctuates about” the tube path suggests that it might be described as the *mean position* of the monomers; in particular, we could define a (tube) path $\hat{\mathbf{r}}(l)$ as the mean position of monomer l for $0 \leq l \leq N$. This immediately raises the question of how this average position should be calculated and, in particular, over what time scale should one take the average, given that the tube is a transient object. The tube model does suggest an answer, at the scaling level, to this question.² At time scales smaller than the entanglement time, τ_e , motion of the chain is considered to be dominated by Rouse motion, such that the typical distance traveled by a monomer in time t is of order $a(t/\tau_e)^{1/4}$. Hence, we anticipate that, if the average position of a monomer is taken over a time $\Delta t_{av} < \tau_e$, then the path so obtained would have persistence length scaling as $a(\Delta t_{av}/\tau_e)^{1/4}$. At time scales immediately larger than the entanglement time (but less than the chain Rouse time, τ_R) entanglements suppress motion perpendicular to the tube path, but 1D Rouse motion along the tube path (which itself is a random walk in three-dimensional space) is permitted. The typical distance in 3D space traveled by a monomer in time t then scales as $a(t/\tau_e)^{1/8}$, and a mean path obtained with averaging time $\tau_e < \Delta t_{av} < \tau_R$ should have persistence length scaling as $a(\Delta t_{av}/\tau_e)^{1/8}$. So, the tube model suggests a time scale τ_e , which marks the transition from sub-tube diameter motion to motion along the tube path. This time scale could, in principle, be obtained by examining the crossover in scaling regimes for the persistence length of a mean path obtained as a function of averaging time. Whether this is practically possible in, for example, a molecular simulation of entangled chain motion remains an open question and is a test of the physics implied by the tube model itself.

In this paper we are concerned primarily with the effect such considerations have on the structure of the equations for constraint release. To this end, we restrict ourselves to a simple model for localization of monomers in the tube in which the averaging is well defined and so which avoids the subtle issues alluded to above (it also has the advantage of being mathematically tractable). In (what has become known as) the Warner–Edwards model^{16–18} (originally designed to describe localization of chains in polymer networks, and based in fact on the earlier work of Deam and Edwards¹⁹) each monomer l along a chain, at position $\mathbf{r}(l)$, is considered to be localized by a harmonic potential centered at $\mathbf{R}(l)$, so that the free energy is given by

$$F = \frac{3}{2b^2} \left[\sum_l (\mathbf{r}(l+1) - \mathbf{r}(l))^2 + \frac{1}{N_s} (\mathbf{r}(l) - \mathbf{R}(l))^2 \right] \quad (3)$$

where b is the monomer step length and the strength of the potential is parametrized by N_s (one may consider the localizing potential be represented by a virtual anchoring chain with N_s monomers).

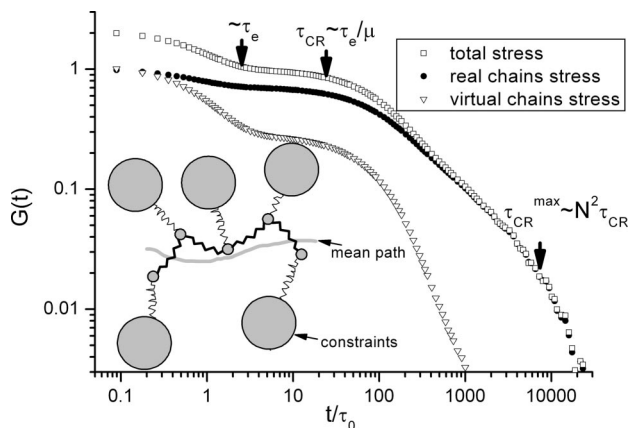


Figure 1. Linear stress relaxation of the “comb” model of constraint release, for $N = 20$, $\mu = 0.03$, $N_s = 0.25$, and $b = 1$.

We note that the positions $\mathbf{R}(l)$ of the localizing potentials do not constitute a smooth path and are thus not a candidate for the “tube path”. It follows directly from the free energy (3) that, at equilibrium, the positions $\mathbf{R}(l)$ must be chosen such that $\langle (\mathbf{R}(l) - \mathbf{r}(l))^2 \rangle = N_s b^2$ but also that there is no correlation between the vectors $\mathbf{R}(l) - \mathbf{r}(l)$ on adjacent monomers. Hence, the equilibrium path described by $\mathbf{R}(l)$ is *less* smooth than that of the chain itself. Any other choice for the statistics of the positions $\mathbf{R}(l)$ of the harmonic potentials (e.g., choosing $\mathbf{R}(l)$ to be a smooth path) does not yield the correct Gaussian random walk statistics for the localized chains. This is discussed in some detail in ref 17.

Defining a “Microscopic” Model. In what follows, we shall proceed by defining a hierarchy of stochastic models related to the Warner–Edwards model, through which we shall test our coarse-graining procedure. In parallel with this, we shall perform the necessary analytical work to assist the coarse-graining and eventually to derive a constitutive model. In our most “microscopic” model, the positions of anchoring points $\mathbf{R}(l)$ (which must somehow define the tube) are moved slowly to represent constraint release.

The model is schematically shown in the inset of Figure 1. It is a usual Rouse chain (with number of beads N , bead friction ζ_0 , and Kuhn step b), but each monomer has an additional bead (with friction ζ_a) attached to it by a virtual chain containing N_s monomers. We require $\mu = \zeta_0/\zeta_a \ll 1$. The linear stress relaxation of the model can be obtained by simple Brownian dynamics simulations using the fluctuation–dissipation theorem. Figure 1 shows the relaxation of the stress arising from the polymer chain itself (filled circles), from the virtual springs connecting the chain to the anchoring points (triangles), and the total stress relaxation (squares). In the remainder of the paper we will follow the usual tube theory assumption that the only contribution to the stress tensor comes from real chains, thus assuming that the filled circles represent the system response. We note that if one uses the fluctuation–dissipation theorem for calculation of component relaxations, cross-correlations have to be taken into account.²⁰ For the illustration purpose, we choose the following simulation parameters— $N = 20$, $\mu = 0.03$, $N_s = 0.25$, $b = 1$ —and define $\tau_0 = \zeta_0(3\pi^2)^{-1}$. The result of the simulation clearly shows a two-step relaxation: fast relaxation of the chain toward its mean position at fixed anchoring points and slow Rouse-like relaxation due to the motion of anchoring points. Thus, it is desirable to identify the slow variables and coarse-grain the fast variables out of the system. As we show below, for the present model it is possible to do it exactly.

Coarse-Grained “Tube” Variables. It is straightforward to find the mean path, $\hat{\mathbf{r}}(l)$, which is the average position of monomer l given that the $\mathbf{R}(l)$ are fixed. This is obtained from

eq 3 by requiring

$$\frac{\partial F}{\partial \mathbf{r}(l)} = 0 \quad \text{at} \quad \mathbf{r}(l) = \hat{\mathbf{r}}(l)$$

which yields

$$\mathbf{R}(l) = \hat{\mathbf{r}}(l) - N_s(\hat{\mathbf{r}}(l+1) + \hat{\mathbf{r}}(l-1) - 2\hat{\mathbf{r}}(l)) \quad (4)$$

The advantageous fact about this model is that the free energy (3) can be separated into the sum of two independent contributions: one depending only on the mean path $\hat{\mathbf{r}}(l)$ and another depending only on fluctuations $\Delta(l) = \mathbf{r}(l) - \hat{\mathbf{r}}(l)$ about the mean path:

$$F = \frac{3}{2b^2} \sum_l \left[(\Delta(l+1) - \Delta(l))^2 + \frac{1}{N_s} (\Delta(l))^2 \right] + \frac{3}{2b^2} \sum_l [(\hat{\mathbf{r}}(l+1) - \hat{\mathbf{r}}(l))^2 + N_s(\hat{\mathbf{r}}(l+1) + \hat{\mathbf{r}}(l-1) - 2\hat{\mathbf{r}}(l))^2] \quad (5)$$

From this it is apparent that, if one were to consider the mean path $\hat{\mathbf{r}}(l)$ to be the relevant slow dynamical variable (and integrate over the “fast” variables $\Delta(l)$), then the path $\hat{\mathbf{r}}(l)$ should behave as though it has a free energy

$$F_{\text{mean path}} = \frac{3}{2b^2} \sum_l [(\hat{\mathbf{r}}(l+1) - \hat{\mathbf{r}}(l))^2 + N_s(\hat{\mathbf{r}}(l+1) + \hat{\mathbf{r}}(l-1) - 2\hat{\mathbf{r}}(l))^2] \quad (6)$$

This free energy contains the usual Gaussian chain stretching energy, but also a term (involving the discrete equivalent of the square of a second derivative) penalizing bending of the mean path. This expression has been obtained from a very simplified model for chain localization, but we believe the observation to be more general: we submit that, if one is to think of the tube path as in some way being the average position of the chain, then this path behaves as a *random walk with a bending energy*, and this is related to the tube path being a smooth path in space.

For the development of a tube constitutive model, it is convenient to rewrite eq 6 in terms of continuous, rather than discrete, coordinates and also to rescale the equations so that they are written in tube, rather than chain, parameters. In fact, changing to a continuous contour variable and differentiating over it is only possible because the tube is now a smooth curve with well-defined length. In tube models there is an “entanglement degree of polymerization” N_e , usually defined from the plateau modulus (although one might also define it in terms of the typical distance of monomer fluctuations or in terms of a persistence length of the tube). We anticipate a rescaling between chain coordinate l and tube coordinate s of form $l = sN_e$ and also note that, given N_e , one can define a tube diameter $a = N_e^{1/2}b$.

Using $l = sN_e$ in eq 6, setting $a = N_e^{1/2}b$, and approximating the sum as an integral gives

$$F = \frac{3}{2a^2} \int ds \left[\left(\frac{\partial \hat{\mathbf{r}}}{\partial s} \right)^2 + \frac{N_s}{N_e^2} \left(\frac{\partial^2 \hat{\mathbf{r}}}{\partial s^2} \right)^2 \right] \quad (7)$$

One can now imagine representing a given polymer (with given tube diameter) through a set of successively fine-grained models, in which the total number of beads N (and thus the number of beads per entanglement, N_e) is increased by a factor α , i.e.

$$\begin{aligned} N &\rightarrow \alpha N \\ N_e &\rightarrow \alpha N_e \\ b &\rightarrow \alpha^{-1/2} b \end{aligned}$$

At the coarse-grained level of the tube diameter, eq 7 should be unaffected by this rescaling; i.e., we require N_s/N_e^2 to remain constant, so that

$$N_s \rightarrow \alpha^2 N_s$$

is the correct way to rescale the localizing potentials (we note that, since the monomer step length b also changes, the strength of the localizing potential *per bead*, which is $3/N_s b^2$, decreases by a factor α).

Varying the factor

$$\kappa = \frac{N_s}{N_e^2} \quad (8)$$

simply adjusts the numerical prefactors in the relationships between the parameter a (or, equivalently, N_e) and quantities such as tube persistence length, distance of monomer fluctuations, and plateau modulus (that is, the value of κ depends on how you define tube diameter from these quantities). We shall suggest an appropriate value for κ later by fixing the relationship between plateau modulus and N_e .

For the sake of clarity, in the main text of the paper we shall present results in terms of these continuous tube coordinates. Nevertheless, for comparison with simulations such as Figure 1 it is useful to have the equivalent results for discrete coordinates, written in terms of the fundamental simulation variables N_s and b ; we present the equivalent results in this form in Appendix A.

It is shown in Appendix B that, at equilibrium, the tube tangent correlation function is

$$\left\langle \frac{\partial \hat{\mathbf{r}}_\alpha}{\partial s} \frac{\partial \hat{\mathbf{r}}_\beta}{\partial s'} \right\rangle = \frac{a^2}{6\sqrt{\kappa}} \exp\left(-\frac{|s-s'|}{\sqrt{\kappa}}\right) \delta_{\alpha\beta} \quad (9)$$

Although this is similar in form to the equilibrium tube path described above for the models of Graham et al.¹² and Read,¹³ it is set by the free energy rather than stochastic noise of constraint release hops.

We additionally note that though, on average, $\langle (\partial \hat{\mathbf{r}}/\partial s) \cdot (\partial \hat{\mathbf{r}}/\partial s) \rangle = a^2/(2\sqrt{\kappa})$, there are fluctuations in the value of $(\partial \hat{\mathbf{r}}/\partial s) \cdot (\partial \hat{\mathbf{r}}/\partial s)$ along the chain. So, the rescaled variable s does not measure the physical *path length* along the tube but remains a rescaled chain monomer coordinate. Furthermore, the number of monomers per unit length of the path defined by $\hat{\mathbf{r}}$ is not constant, but varies along the chain.

Similarly, one can show that the fluctuations $\Delta(s)$ about the mean path obey

$$\langle \Delta_\alpha(s) \Delta_\beta(s') \rangle = \frac{a^2 \sqrt{\kappa}}{6} \exp\left(-\frac{|s-s'|}{\sqrt{\kappa}}\right) \delta_{\alpha\beta} \quad (10)$$

Verifying the Slow Variables via Simulation. At this point we can check, by simulations, our assumption that $\hat{\mathbf{r}}$ is the relevant slow dynamical variable. At every time step of the simulation outlined above, we calculate (in discrete coordinates l) the position of the mean-path $\hat{\mathbf{r}}(l)$ given by the set of anchoring points $\mathbf{R}(l)$ using the inverse of eq 4 for a finite chain. Then, in principle, we should be able to calculate the stress at long times using $\hat{\mathbf{r}}(l)$ only. The natural question to ask is what should be the expression for the stress tensor as a function of $\hat{\mathbf{r}}$; i.e., do we have to include bending energy in the calculation? Applying a virtual-work argument, and assuming a system volume of V , the free energy eq 7 corresponds to the stress tensor

$$\begin{aligned} \sigma_{\alpha\beta} &= \frac{k_B T}{V} \sum_{\text{chains}} \frac{3}{a^2} \int_0^{N/N_e} ds \left(\frac{\partial \hat{\mathbf{r}}_\alpha}{\partial s} \frac{\partial \hat{\mathbf{r}}_\beta}{\partial s} + \kappa \frac{\partial^2 \hat{\mathbf{r}}_\alpha}{\partial s^2} \frac{\partial^2 \hat{\mathbf{r}}_\beta}{\partial s^2} \right) \\ &= \sigma_{\alpha\beta}^{\text{Kramers}} + \sigma_{\alpha\beta}^{\text{bending}} \end{aligned} \quad (11)$$

where the first term is usual Kramers expression and the second term comes from additional bending force. However, we do not want to include forces from the virtual springs into the real

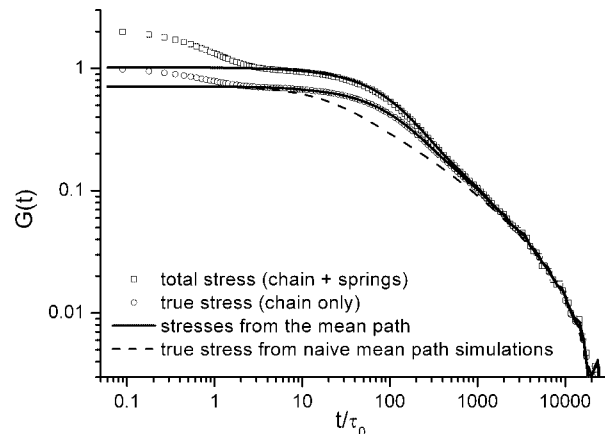


Figure 2. Comparison of exact stress relaxation (same as Figure 1) with the stress relaxation calculated from mean paths only (thick lines). The dashed line shows results of naive mean path simulations where friction on the mean path is assigned to each bead independently.

stress tensor. Figure 2 shows comparison of the stress relaxation of the full model and stress relaxation obtained from the mean path. We find that the total comb stress relaxation agrees with the relaxation of stress given by eq 11 after some time of order τ_e , whereas the real chain stress relaxation agrees with the relaxation of $\sigma_{\alpha\beta}^{\text{Kramers}}$ of eq 11. Note that in the simulations we use equilibrium fluctuations to calculate relaxation functions: for this, cross-correlations have to be taken into account in the manner of Ramirez et al.,²⁰ so that for example $G^{\text{Kramers}}(t) = (V/k_B T) \langle (\sigma_{\alpha\beta}^{\text{Kramers}}(t) \sigma_{\alpha\beta}^{\text{Kramers}}(0)) + \langle \sigma_{\alpha\beta}^{\text{Kramers}}(t) \sigma_{\alpha\beta}^{\text{bending}}(0) \rangle \rangle$.

The exact agreement of the stresses obtained from fine-grained and from coarse-grained variables gives us assurance that, once we modeled the motion of the mean path correctly, the stress will also be predicted correctly. In particular, we would like to be able to do away with the chain coordinates altogether and just simulate the motion of the mean path. We can attempt to perform this straight away by assigning a friction (and associated noise) to each point of $\hat{\mathbf{r}}(l)$ and calculate regular forces from the free energy eq 6. The result for the real stress relaxation is shown in Figure 2 by the dashed line. Although it agrees with the true stress relaxation at the terminal time (after selecting an appropriate friction for $\hat{\mathbf{r}}(l)$ points $\zeta_{\hat{\mathbf{r}}} = \zeta_a$), there is a noticeable disagreement at earlier times of order of the constraint release time. In the linear regime this is around the reptation time and thus has to be treated accurately by the tube theory, whereas the terminal time of our model is usually not relevant experimentally since the tube is usually destroyed by reptation (a counterexample is binary mixtures of very long by very dilute polymers, where terminal time is controlled by constraint release).²¹ Thus, a more accurate model for dynamics of the mean path is required: we cannot simply assume uncorrelated noise on each bead of $\hat{\mathbf{r}}(l)$.

A second conclusion from this exercise is that, if one assumes that the total stress comes from chains only (and not virtual springs) then the appropriate expression for the stress from the $\hat{\mathbf{r}}$ variable is simply

$$\sigma_{\alpha\beta} = \frac{k_B T}{V} \sum_{\text{chains}} \frac{3}{a^2} \int_0^{N/N_e} ds \left(\frac{\partial \hat{\mathbf{r}}_\alpha}{\partial s} \frac{\partial \hat{\mathbf{r}}_\beta}{\partial s} \right) \quad (12)$$

A similar conclusion can be drawn by noting that, for a chain equilibrated at fixed $\hat{\mathbf{r}}$

$$\begin{aligned} \langle (r_\alpha(l+1) - r_\alpha(l))(r_\beta(l+1) - r_\beta(l)) \rangle &= \\ \langle (\hat{\mathbf{r}}_\alpha(l+1) - \hat{\mathbf{r}}_\alpha(l))(\hat{\mathbf{r}}_\beta(l+1) - \hat{\mathbf{r}}_\beta(l)) \rangle &+ \\ \langle (\Delta_\alpha(l+1) - \Delta_\alpha(l))(\Delta_\beta(l+1) - \Delta_\beta(l)) \rangle & \end{aligned} \quad (13)$$

and recognizing that, for isotropic confining potentials, the second term contributes only an isotropic pressure.

One can now consider applying a step shear strain γ to a set of equilibrated mean paths, so that the new position $\mathbf{f}(s)$ of the tube is given from the original equilibrium position $\mathbf{f}^0(s)$ via

$$(\hat{r}_1, \hat{r}_2, \hat{r}_3) = (\hat{r}_1^0 + \gamma \hat{r}_2^0, \hat{r}_2^0, \hat{r}_3^0)$$

Thus

$$\begin{aligned} \left\langle \frac{\partial \hat{r}_1}{\partial s} \frac{\partial \hat{r}_2}{\partial s} \right\rangle &= \left\langle \frac{\partial \hat{r}_1^0}{\partial s} \frac{\partial \hat{r}_2^0}{\partial s} \right\rangle + \gamma \left\langle \frac{\partial \hat{r}_2^0}{\partial s} \frac{\partial \hat{r}_2^0}{\partial s} \right\rangle \\ &= \frac{\gamma a^2}{6\sqrt{\kappa}} \end{aligned}$$

where we have used eq 9 for averaging the equilibrium position $\mathbf{f}^0(s)$. Then, substituting into eq 12 gives an average shear stress of

$$\sigma_{12} = \frac{k_B T}{V} n_c \frac{N}{N_e} \frac{1}{2\sqrt{\kappa}} \gamma = \frac{C k_B T}{N_e} \frac{1}{2\sqrt{\kappa}} \gamma \quad (14)$$

where n_c is the total number of chains and C is the monomer concentration. The usual definition of N_e is from the modulus, via $G = C k_B T / N_e$ (we here ignore factors of 4/5 arising from equilibration by chain motion along the tube—we have no along-tube motion in the model as yet). This suggests that, if the N_e we introduced above (initially as a rescaling variable from l to s) is to be the conventional “entanglement degree of polymerization”, then $2\sqrt{\kappa} = 1$, i.e., $\kappa = 1/4$, and

$$N_e = 2N_s^{1/2} \quad (15)$$

We note also that this leads to

$$\left\langle \frac{\partial \mathbf{f}}{\partial s} \frac{\partial \mathbf{f}}{\partial s} \right\rangle = a^2 \quad (16)$$

and

$$\langle \Delta(s) \cdot \Delta(s) \rangle = \frac{a^2}{4} \quad (17)$$

From the latter, one might (optimistically) suggest that the tube radius, d , is obtained from $d = (\langle \Delta(s) \cdot \Delta(s) \rangle)^{1/2}$, giving a tube diameter of $2d = a$! For the remainder of the paper, we shall use $\kappa = 1/4$ (but note that other choices of κ are effectively just different definitions of N_e).

Constraint Release in a Tube with Bending Energy. We envisage a constraint release event as giving the opportunity for a “hop” in the tube path, $\mathbf{f}(s)$. We consider a possible hop of general form

$$\mathbf{f}(s, t^+) - \mathbf{f}(s, t) = \mathbf{h}(s) \quad (18)$$

where the hop is described by an envelope function $\eta(s - s_m)$ centered on s_m and a hop vector \mathbf{H} :

$$\mathbf{h}(s) = \mathbf{H} \eta(s - s_m)$$

with $\langle H_\alpha H_\beta \rangle = h^2 \delta_{\alpha\beta}$. We assume the envelope function to be normalized, i.e., $\int \eta(s - s_m) ds = 1$. If we allow such hops to be accepted (or not) on the principle of detailed balance, and average over the position and size of such hops, then we can show (see Appendix C) that the path $\mathbf{f}(s)$ obeys a dynamical equation of form

$$\frac{\partial \mathbf{f}(s)}{\partial t} = \dots + \frac{3h^2 \bar{\nu}}{4a^2} \int \psi(s - s') \left[\frac{\partial^2 \mathbf{f}}{\partial s'^2} - \frac{1}{4} \frac{\partial^4 \mathbf{f}}{\partial s'^4} \right] ds' + \mathbf{g}(s, t) \quad (19)$$

where the noise has statistics

$$\langle g_\alpha(s, t) g_\beta(s', t') \rangle = \frac{h^2 \bar{\nu}}{2} \psi(s - s') \delta(t - t') \delta_{\alpha\beta} \quad (20)$$

and the function ψ is related to the envelope function η via

$$\psi(s - s') = \int \eta(s - s_m) \eta(s' - s_m) ds_m$$

$\bar{\nu}$ is the rate of such hop attempts per entanglement length (i.e., per unit of s).

Equations 19 and 20 are our equivalent to eqs 1 and 2 but are in continuous rather than discrete coordinates. We make two observations about the new equation. First, the function $\psi(s - s')$, representing a finite-width noise function, is also present in the dissipative relaxation term. This indicates consistency with the fluctuation–dissipation theorem. Second, there is an extra term (involving the fourth derivative) due to the bending energy of the mean path. This term ensures that, irrespective of the mathematical form of the envelope function η for the noise, the equilibrium tube configuration under the action of eq 19 is as given by eq 9, i.e., the equilibrium obtained from the free energy. These two observations contrast with the previous models of Graham et al.¹² and Read¹³ and are the result of (i) starting from a free energy which gives a smooth tube path and then (ii) deriving dynamical equations using a detailed balance argument.

In our stochastic model, constraint release events involve motion of the localizing potentials. This provides a natural choice for the envelope function which we derive in Appendix D by considering the change in the mean path when one of the localizing potentials, centered on s_m , is moved, yielding

$$\eta(s - s_m) = \exp(-2ls - s_m) \quad (21)$$

At this stage, it is worth commenting on the absence of the factor $1/\lambda$ in the equations obtained here (cf. Graham et al.¹² and see the discussion in section 2). In our model (and in the original Warner–Edwards model),¹⁶ each monomer is attached to a localizing spring, and the number of these springs does not change as the chain stretches (if we did increase the number of springs, then the typical fluctuation distance of the chain about the mean path would decrease). We consider constraint release events to be equivalent to the movement of these localizing constraints, and since the number of constraints per monomer remains fixed, there is no rescaling of the equations due to chain stretch. This serves to highlight an important difference between the description of a tube in terms of localizing potentials on monomers and a description in terms of a set of stiff, straight “tube segments” (which was the conceptual picture in Graham et al.¹² and Doi and Edwards).² Below, we shall demonstrate that the qualitative behavior of the system of equations is relatively insensitive to the particular choice of $\psi(s)$ (via $\eta(s)$) within reasonable limits, but also that the choice (21) gives results that are quantitatively very close to those of the model of Graham et al. (2003), but without needing to invoke the $1/\lambda$ rescaling due to stretch.

Stochastic Simulations of the Mean Path. We are now in position to perform coarse-grained simulations of the mean path eq 19 and compare them to the fine-grained model. In these simulations, to generate correlated random forces satisfying eq 20, we first generate independent random displacement of anchoring points and then get the corresponding displacements by inverting eq 4 (in discrete coordinates). The results are shown in Figure 3 by solid lines, exhibiting perfect agreement with the fine-grained model after initial relaxation time τ_e .

Thus, we conclude that if one defines the tube coordinate as the averaged chain position over fast fluctuations (averaging time around τ_e), the tube free energy has to have a bending energy term, and the random forces due to constraint release have to have finite correlation length along the chain. In case

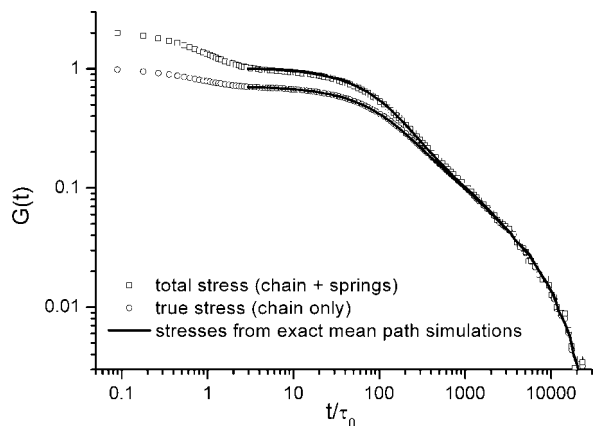


Figure 3. True stress relaxation (same as Figure 1) compared with results from exact mean path simulations.

of no slip of the virtual springs (pure constraint release with no reptation and no contour length fluctuations) this averaging can be performed exactly. However, we hope that the general conclusions will still hold with the slip between entanglements. Thus, we proceed to modify the constitutive equation for the tube model.

Constitutive Model. The constitutive equation obtained by Graham et al.¹² was written in terms of a dynamical equation for the quantity $f_{\alpha\beta}(s, s') = (1/a^2)\langle(\partial\hat{r}_\alpha/\partial s)(\partial\hat{r}_\beta/\partial s')\rangle$. Following the same approach, and making use of eq 38 from Appendix B, we obtain the constraint release contribution to the dynamics of this variable as

$$\begin{aligned} \frac{\partial f_{\alpha\beta}(s, s')}{\partial t} = & \dots + \\ & \frac{3\nu}{2} \int ds'' \left[\psi(s-s'') \left(\frac{\partial^2 \tilde{f}_{\alpha\beta}(s'', s')}{\partial s''^2} - \frac{1}{4} \frac{\partial^4 \tilde{f}_{\alpha\beta}(s'', s')}{\partial s''^4} \right) + \right. \\ & \left. \psi(s'-s'') \left(\frac{\partial^2 \tilde{f}_{\alpha\beta}(s, s'')}{\partial s''^2} - \frac{1}{4} \frac{\partial^4 \tilde{f}_{\alpha\beta}(s, s'')}{\partial s''^4} \right) \right] \\ = & \dots + \\ & \frac{3\nu}{2} \int ds'' \left[\frac{\partial^2 \psi(s-s'')}{\partial s''^2} \left(\tilde{f}_{\alpha\beta}(s'', s') - \frac{1}{4} \frac{\partial^2 \tilde{f}_{\alpha\beta}(s'', s')}{\partial s''^2} \right) + \right. \\ & \left. \frac{\partial^2 \psi(s'-s'')}{\partial s''^2} \left(\tilde{f}_{\alpha\beta}(s, s'') - \frac{1}{4} \frac{\partial^2 \tilde{f}_{\alpha\beta}(s, s'')}{\partial s''^2} \right) \right] \quad (22) \end{aligned}$$

where $\tilde{f}_{\alpha\beta} = f_{\alpha\beta} - f_{\alpha\beta}^{\text{eq}}$, with the equilibrium $f_{\alpha\beta}^{\text{eq}}$ being given by

$$f_{\alpha\beta}^{\text{eq}}(s, s') = \frac{\delta_{\alpha\beta}}{3} \exp(-2|s-s'|) \quad (23)$$

The rescaled hop rate ν is the effective rate of successful hops of distance of order the tube diameter, a , i.e. $h^2\tilde{\nu} = 2a^2\nu$, and is equivalent to the hop rate used by Graham et al.

The equivalent equation to (22) in discrete, simulation coordinates is given in eq 33 of Appendix A. In this discrete case we can numerically solve this system of $N \times N$ equations (for $0 \leq l, l' \leq N-1$) following a rapid step strain, to obtain the relaxation modulus $G(t)$. We compare this against the stochastic simulation results in Figure 4. The result is indistinguishable from the results of the Brownian dynamics simulations. This is despite the fact that the function ψ is obtained for infinite chains (i.e., ignoring boundary conditions), suggesting that boundary conditions are relatively unimportant for the particular choice of simulation parameters. For this particular model, then, we have shown it is possible to perform Brownian dynamics simulations, choose an appropriate set of coarse-

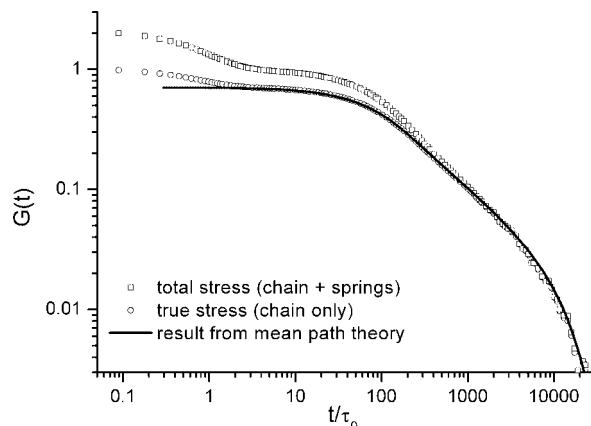


Figure 4. True stress relaxation (same as Figure 1) compared with results from exact mean path theory.

grained variables (in this case the mean path), perform stochastic simulations at the level of the coarse-grained variables, and, finally, obtain a constitutive model.

We are now in a position to make use of our new description of the constraint release dynamics within a more detailed constitutive model for entangled linear polymers. For the sake of (relative) simplicity, we replace the constraint release terms in the model of Graham et al. with eq 22 but leave the remaining terms (for flow, reptation, chain retraction, etc.) unchanged. Our argument for doing this is a purely pragmatic one: these remaining terms do not appear to suffer from the same issues of oversensitivity toward the precise choice of parameters as did the constraint release term. This being said, we should highlight two outstanding issues whose solution is beyond the present work. First, it seems clear that the higher derivatives due the bending energy should also change the form of the retraction (stretch relaxation) term and will presumably affect the high-frequency Rouse modes for along-tube motion (they might also affect the equilibrium tube contour length in a tube which has been oriented by flow). Detailed consideration of this issue would need a reassessment of the closure approximations used by Graham et al. for their retraction term and should probably also include a description of the stochastic noise associated with the along-tube motion (Graham et al. restricted the stochastic noise to just the reptation mode).

A second issue concerns the expression used for the stress. Following the discussion at the end of section 3, we use (in line with Graham et al.)

$$\sigma_{\alpha\beta} = \frac{3G_0}{Z} \int_0^Z ds f_{\alpha\beta}(s, s) = \frac{12G_e}{5Z} \int_0^Z ds f_{\alpha\beta}(s, s) \quad (24)$$

where $Z = N/N_e$ is the number of entanglement lengths in a chain. As indicated above, this is based on the (unverified) assumption that the stress comes only from the chains (and that the localizing potentials, which represent confining effect of surrounding chains, contribute to the stress only to the extent that they restrict the chain configurations). In the case of networks, this issue has been resolved by Rubinstein and Panyukov,^{22,23} who demonstrated that, if the localizing potentials deform in a particular manner with the applied strain, the stress obtained from the derivatives of the free energy *including* the harmonic potentials is the same as that obtained from the chain stress expression $\langle(\partial r_\alpha/\partial s)(\partial r_\beta/\partial s)\rangle$. However, to extend this concept to melts does not appear trivial (to us): it requires an additional dynamical equation for the anisotropy of the localizing potentials, with an assumption as to how (and on what time scale) these relax back toward equilibrium.

Appendix E gives details of the boundary conditions we use for the chain ends.

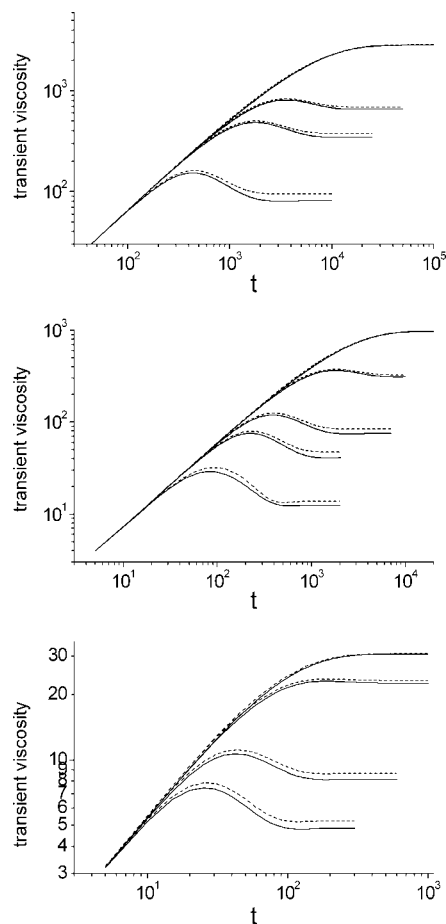


Figure 5. Comparison of the shear viscosity predictions of the current work (solid lines) with those of the model of Graham et al. (2003) (dashed lines), for models with $\tau_e = 1.0$ and $G_e = 1.0$. Top: $Z = 20$, shear rates 10^{-5} , 5×10^{-4} , 10^{-3} , 5×10^{-3} . Middle: $Z = 15$, shear rates 5×10^{-5} , 10^{-3} , 5×10^{-3} , 10^{-2} , 5×10^{-2} . Bottom: $Z = 6$, shear rates 10^{-3} , 10^{-2} , 10^{-1} , 5×10^{-1} .

4. Results and Discussion

The shear viscosity predictions during start-up shear flow of the constitutive model with bending energy are shown in Figure 5, for $Z = 6$, 15, and 20, for a wide range of shear rates. Also shown in the figures are (using identical parameters) predictions of the model of Graham et al.,¹² which has been previously shown to be in good agreement for a wide range of experimental data. The predictions of the new model agree reasonably well with those of the model of Graham et al. and are certainly within the level of agreement between their model and experimental data. We can state, with confidence, that any data which is well described by Graham et al. will be equally well described by the present modification of that model. We emphasize, however, that in the present model we do not need to invoke the $1/\lambda$ rescaling of the constraint release terms due to stretch—this appears to be a result of a combination of the bending energy term and the smoother noise function in the dynamical equations.

We are also able to demonstrate that the present model does not show the same sensitivity toward the choice of the noise function as discussed in Read¹³ for the Graham et al. model. Figure 6 shows shear viscosity predictions for different choices of the function $\psi(s)$ (via $\eta(s)$), for $Z = 15$, for two different shear rates (above and below the inverse of the stretch relaxation time). These figures show results for the exponential form for $\eta(s)$ (as given in eq 15) and, for Gaussian forms, given by $\eta(s) = (\theta/\pi)^{1/2} \exp(-\theta(s - s_m)^2)$ in which the width is varied via the parameter θ . In the previous model such variation of the

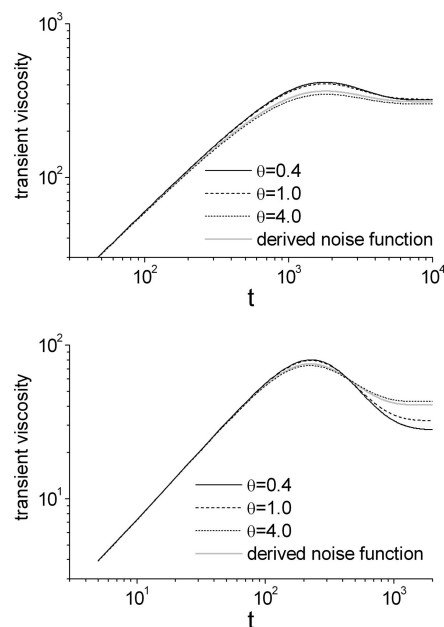


Figure 6. Shear viscosity predictions for $Z = 15$, $G_e = 1$, and $\tau_e = 1$ and (top) $\dot{\gamma} = 10^{-3}$, i.e., $\dot{\gamma}\tau_R = 0.225$ and (bottom) $\dot{\gamma} = 10^{-2}$, i.e., $\dot{\gamma}\tau_R = 2.25$. We show results for different forms of $\psi(s)$ (via $\eta(s)$). The different values of θ correspond to Gaussian forms of $\eta(s - s_m)$ given by $(\theta/\pi)^{1/2} \exp(-\theta(s - s_m)^2)$ and “derived noise function” corresponds to $\eta(s - s_m)$ given by $\exp(-2|s - s_m|)$.

noise function would have resulted in qualitatively different results. Here, although there are naturally quantitative differences as the width of the noise function is varied, the *qualitative* behavior of the shear stress during start up (i.e., the presence of the stress overshoot followed by the steady state) remains fixed and is relatively independent of the particular choice of $\eta(s)$. We believe that this robustness toward choice of the noise function occurs because the equilibrium configuration of the tube is now determined by the free energy rather than the noise function.

These results indicate, then, that although qualitative behavior of the present model is not sensitive to the choice of the noise function, the particular choice of eq 21 (which appears to be the natural choice arising from the underlying model, as discussed above) gives results which are in good agreement with the Graham et al. model and thus with experimental data.

In extensional flows of monodisperse polymers, constraint release has only a weak effect. In fact, since the tube rapidly becomes stretched and aligned in the extension direction, constraint release hops tend to add “kinks” to the tube, thus increasing its length and contributing to chain stretch. Nevertheless, the dominant contributions to the dynamics come from a balance between chain stretch in the extensional flow and stretch relaxation via chain retraction along the tube; constraint release serves only to adjust this balance slightly. Thus, when comparing our modified model with the original one of Graham et al., we see a small difference in the extension rate at the onset of strain hardening (the onset extension rate in our model is fractionally higher; equivalently, the Graham et al. model gives marginally higher stresses at the same extension rate).

5. Conclusion

We have investigated the idea that the “tube” in theories of entangled chain dynamics might be thought of as the path of the *mean positions* of the chain monomers. Applying this idea to the simple Warner–Edwards model for the tube, we showed that such a path behaves as though it has a bending energy and that this is related to the tube path being a smooth path in space.

Although the bending energy term was derived from a very simple model of the tube, we suspect that a term of this form is more general and that in other models it might represent the first in a series of additional terms involving higher derivatives.

Beginning with the Warner–Edwards model, we defined a microscopic stochastic model in which the positions of the confining potentials were moved to simulate constraint release. We were able to show by stochastic simulations that, at least for this simple model, the mean path provides an appropriate (and in this case exact) route to coarse-graining. The long-time dynamics and stress response could be specified in terms of the mean path alone. Finally, a constitutive model could be derived which matched the simulation results exactly.

We investigated the consequences of modifying the (convective) constraint release dynamics in the Graham et al.¹² model to include the new term with correlated noise and bending energy. In particular, we noted that the (smooth) equilibrium configuration of the tube was now set by the underlying free energy rather than the stochastic noise. Predictions of stress during start-up shear flow from the resulting set of equations were in good agreement with those of Graham et al., but without the need to invoke the $1/\lambda$ rescaling of the constraint release terms due to stretch (which has the ambiguities discussed in section 2). The resulting equations are also much less sensitive to the form and width of the stochastic noise function, but the underlying physical model suggests a natural choice for the noise function which gives good agreement with the Graham et al. model.

From the point of view of having a set of equations which give good agreement with experimental data, the present work makes no advances beyond the model of Graham et al.¹²—and, in fact, the equations obtained are computationally more expensive to solve! Still, we consider that the agreement of our predictions with those of the model of Graham et al. to be a positive result of this work; it was by no means guaranteed, yet without this, our predictions would deviate from experimental data. But, by placing the model on a sounder physical basis, progress has been made in three ways: (i) we have removed the problems with the model discussed by Read,¹³ i.e., the sensitivity to the noise function and issues with the $1/\lambda$ rescaling of the constraint release terms, (ii) the concept of the tube as a *mean path* of the monomers is one which can be tested by more detailed molecular simulation and may allow coarse-graining from simulations (indeed, we have demonstrated such a coarse-graining in one simple case), and (iii) the underlying model is one that can be extended to deal with more complicated situations (such as the multiple constraint release rates present in polydisperse or branched polymer systems). We anticipate the latter two points will form the basis of future extensions of this work.

Acknowledgment. The authors gratefully acknowledge the financial support of the EPSRC for this work via the Microscale Polymer Processing project and Advanced Research Fellowships (A.E.L. and D.J.R.).

Appendix A. Results for Discrete Coordinates

In this appendix we present, for discrete chain coordinates and simulation variables, equivalent results to those in the main text of the paper. The derivation of these results follows essentially the same method given in subsequent appendices for continuous coordinates but requires solution of discrete difference instead of differential equations (but see also the methodology in the Appendix of ref 22). As with the continuous coordinate results, we present for simplicity results in the limit of infinite chains (i.e., ignoring boundary conditions). Here, and in Appendix E, we shall use a convenient shorthand for discrete

differences: for $g(l)$ defined at integer l

$$\frac{\partial g}{\partial l} \equiv g(l+1) - g(l)$$

$$\frac{\partial^2 g}{\partial l^2} \equiv g(l+1) + g(l-1) - 2g(l)$$

$$\frac{\partial^4 g}{\partial l^4} \equiv g(l+2) - 4g(l+1) + 6g(l) - 4g(l-1) + g(l-2)$$

We find the correlation function for the mean path is

$$\left\langle \frac{\partial \hat{r}_\alpha}{\partial l} \frac{\partial \hat{r}_\beta}{\partial l'} \right\rangle = \frac{b^2}{3} \frac{1}{\sqrt{4N_s + 1}} A^{l-l'} \delta_{\alpha\beta} \quad (25)$$

where the quantity A is given by

$$A = \frac{2N_s + 1 - \sqrt{4N_s + 1}}{2N_s} \quad (26)$$

Similarly, the fluctuations about the mean path obey

$$\langle \Delta_\alpha(l) \Delta_\beta(l') \rangle = \frac{b^2}{3} \frac{N_s}{\sqrt{4N_s + 1}} A^{l-l'} \delta_{\alpha\beta} \quad (27)$$

The stress tensor is given by

$$\sigma_{\alpha\beta} = \frac{k_B T}{V} \sum_{\text{chains}} \frac{3}{b^2} \sum_l \left(\frac{\partial \hat{r}_\alpha}{\partial l} \frac{\partial \hat{r}_\beta}{\partial l} \right)$$

from which (following a step shear strain γ from equilibrium and using a similar derivation to eq 14) one obtains a modulus

$$G = \frac{\sigma_{12}}{\gamma} = \frac{C k_B T}{\sqrt{4N_s + 1}} \quad (28)$$

where C is the bead concentration. From this we identify an “entanglement degree of polymerization”

$$N_e = \sqrt{4N_s + 1} \quad (29)$$

In the continuum limit of large N_e and N_s (which corresponds to many beads per entanglement, with weak springs attached to each bead) this agrees with the result given in the main text, but also includes the crossover to small N_s where each spring strongly localizes its bead and the plateau modulus is close to $C k_B T$.

To obtain the dynamical equations for the mean path, we note that if the localizing potential at l_m is moved by \mathbf{H} then the corresponding change in $\hat{\mathbf{r}}$ is

$$\Delta \hat{\mathbf{r}}(l) = \mathbf{H} \frac{A^{l-l_m}}{\sqrt{4N_s + 1}}$$

which suggests a hop profile function

$$\eta(l - l_m) = \frac{A^{l-l_m}}{\sqrt{4N_s + 1}}$$

which is the solution of $[1 - N_s(\partial^2/\partial l^2)]\eta(l - l_m) = \delta_{l-l_m}$. Assigning a friction ζ_a to each anchoring point, we obtain the stochastic equation governing $\hat{\mathbf{r}}$ to be

$$\frac{\partial \hat{\mathbf{r}}(l)}{\partial t} = \frac{3k_B T}{b^2 \zeta_a} \sum_{l'} \psi(l - l') \left[\frac{\partial^2 \hat{\mathbf{r}}}{\partial l'^2} - N_s \frac{\partial^4 \hat{\mathbf{r}}}{\partial l'^4} \right] + \mathbf{g}(l, t) \quad (30)$$

where

$$\langle g_\alpha(l, t) g_\beta(l', t') \rangle = \frac{2k_B T}{\zeta_a} \psi(l - l') \delta_{\alpha\beta} \delta(t - t') \quad (31)$$

and the function

$$\begin{aligned}\psi(l-l') &= \sum_{l_m} \eta(l-l_m) \eta(l'-l_m) \\ &= \frac{A^{l-l'}}{4N_s+1} \left(|l-l'| + \frac{2N_s+1}{\sqrt{4N_s+1}} \right) \quad (32)\end{aligned}$$

From these, we obtain the dynamics of $f_{\alpha\beta}(l, l') = (3/b^2) \langle (\partial \hat{f}_{\alpha\beta} / \partial l) (\partial \hat{f}_{\beta\alpha} / \partial l') \rangle$ to be

$$\begin{aligned}\frac{\partial f_{\alpha\beta}(l, l')}{\partial t} &= \frac{3k_B T}{b^2 \zeta_a} \sum_{l''} \left[\psi(l-l'') \left(\frac{\partial^2 \tilde{f}_{\alpha\beta}(l'', l')}{\partial l''^2} - N_s \frac{\partial^4 \tilde{f}_{\alpha\beta}(l'', l')}{\partial l''^4} \right) + \right. \\ &\quad \left. \psi(l'-l'') \left(\frac{\partial^2 \tilde{f}_{\alpha\beta}(l, l'')}{\partial l''^2} - N_s \frac{\partial^4 \tilde{f}_{\alpha\beta}(l, l'')}{\partial l''^4} \right) \right] \\ &= \frac{3k_B T}{b^2 \zeta_a} \sum_{l''} \left[\frac{\partial^2 \psi(l-l'')}{\partial l''^2} \left(\tilde{f}_{\alpha\beta}(l'', l') - N_s \frac{\partial^2 \tilde{f}_{\alpha\beta}(l'', l')}{\partial l''^2} \right) + \right. \\ &\quad \left. \frac{\partial^2 \psi(l'-l'')}{\partial l''^2} \left(\tilde{f}_{\alpha\beta}(l, l'') - N_s \frac{\partial^2 \tilde{f}_{\alpha\beta}(l, l'')}{\partial l''^2} \right) \right] \quad (33)\end{aligned}$$

where $\tilde{f}_{\alpha\beta}(l, l') = f_{\alpha\beta}(l, l') - f_{\alpha\beta}^{\text{eq}}(l, l')$ and the equilibrium $f_{\alpha\beta}^{\text{eq}}(l, l') = (4N_s+1)^{-1/2} A^{l-l'} \delta_{\alpha\beta}$.

Appendix B. Equilibrium Configuration of Mean Path

Here we investigate the equilibrium configuration of a mean path which has free energy given in eq 7. For simplicity, we allow s to take any real value (corresponding to an infinite tube—we consider the issue of boundary conditions for a finite tube in Appendix E). It is convenient to define a quantity $\mathbf{q}(s) = (1/a)(\partial \mathbf{r}/\partial s)$ and rewrite the free energy as

$$F = \frac{3}{2} \int ds \left[(\mathbf{q}(s))^2 + \kappa \left(\frac{\partial \mathbf{q}}{\partial s} \right)^2 \right] \quad (34)$$

Suppose we fix the value of \mathbf{q} at some value of s ($= 0$, say), i.e., $\mathbf{q}(0) = \mathbf{q}_0$. Then, $\mathbf{q}(s)$ can be written as a sum of a component $\bar{\mathbf{q}}(s)$ correlated with $\mathbf{q}(0)$ plus uncorrelated fluctuations $\Delta \mathbf{q}(s)$:

$$\mathbf{q}(s) = \bar{\mathbf{q}}(s) + \Delta \mathbf{q}(s)$$

with the constraint $\Delta \mathbf{q}(0) = \mathbf{0}$. $\bar{\mathbf{q}}(s)$ can be found from the functional derivative

$$\frac{\delta F}{\delta \mathbf{q}(s)} = 0$$

giving

$$\bar{\mathbf{q}} - \kappa \frac{\partial^2 \bar{\mathbf{q}}}{\partial s^2} = 0$$

which (using the boundary conditions $\bar{\mathbf{q}}(0) = \mathbf{q}_0$ and $\bar{\mathbf{q}}(s) \rightarrow 0$ as $s \rightarrow \pm\infty$) solves to give

$$\bar{\mathbf{q}}(s) = \mathbf{q}_0 \exp\left(-\frac{|s|}{\sqrt{\kappa}}\right) \quad (35)$$

Substituting back into (34) gives the free energy in terms of \mathbf{q}_0 and the fluctuations $\Delta \mathbf{q}(s)$:

$$F = 3\sqrt{\kappa} \mathbf{q}_0^2 + \frac{3}{2} \int ds \left[(\Delta \mathbf{q}(s))^2 + \kappa \left(\frac{\partial \Delta \mathbf{q}}{\partial s} \right)^2 \right] \quad (36)$$

from which is apparent that, at equilibrium

$$\langle q_{0\alpha} q_{0\beta} \rangle = \frac{1}{6\sqrt{\kappa}} \delta_{\alpha\beta}$$

Equation 35 indicates that equilibrium correlations in $\mathbf{q}(s)$ decay along the mean path as $\exp(-|s|/\sqrt{\kappa})$, so that at equilibrium

$$\left\langle \frac{\partial \hat{f}_{\alpha}}{\partial s} \frac{\partial \hat{f}_{\beta}}{\partial s'} \right\rangle = \frac{a^2}{6\sqrt{\kappa}} \exp\left(-\frac{|s-s'|}{\sqrt{\kappa}}\right) \delta_{\alpha\beta} \quad (37)$$

It is useful to note that for the function $\exp(-|s|/\sqrt{\kappa})$

$$\left(1 - \kappa \frac{\partial^2}{\partial s^2} \right) \exp\left(-\frac{|s|}{\sqrt{\kappa}}\right) = 2\sqrt{\kappa} \delta(s-s') \quad (38)$$

Appendix C. Tube Hops from Detailed Balance

In a small interval Δt in time, we consider that a section of tube $0 < s < Z$ undergoes $Z\bar{v}\Delta t$ attempted hops, such that the i th such hop is of form $\mathbf{h}_i(s) = \mathbf{H}_i \eta(s - s_{m,i})$. For small $\mathbf{h}_i(s)$, the change in free energy (from eq 7) is

$$\Delta F_i = -\frac{3}{a^2} \int ds' \mathbf{h}_i(s') \cdot \left[\frac{\partial^2 \mathbf{r}}{\partial s'^2} - \frac{1}{4} \frac{\partial^4 \mathbf{r}}{\partial s'^4} \right]$$

Using the principle of detailed balance, we assume that an attempted hop is “accepted” with probability p_i such that

$$p_i = \frac{\exp(-\Delta F_i)}{1 + \exp(-\Delta F_i)} \approx \frac{1}{2} \left(1 - \frac{\Delta F_i}{2} \right)$$

Hence, in the interval Δt , the change in the tube path due to these hops is

$$\mathbf{r}(s, t + \Delta t) - \mathbf{r}(s, t) = \sum_{i=1}^{Z\bar{v}\Delta t} \mathbf{h}_i(s) y_i$$

where the random variable $y_i = 1$ if the hop is accepted and 0 otherwise. We write this change in tube path in terms of its average and the deviation from the average

$$\mathbf{r}(s, t + \Delta t) - \mathbf{r}(s, t) = \left\langle \sum_{i=1}^{Z\bar{v}\Delta t} \mathbf{h}_i(s) y_i \right\rangle + \mathbf{g}(s, t) \Delta t$$

where the average should be taken over three quantities: the acceptance of the hop ($\langle y_i \rangle = p_i$, $\langle y_i y_j \rangle = p_i \delta_{ij}$), over the hop vector ($\langle H_{i\alpha} H_{j\beta} \rangle = h^2 \delta_{\alpha\beta} \delta_{ij}$) and over the positions of the hop centers, s_m ($\langle \dots \rangle_{s_m} \equiv (1/Z) \int \dots ds_m$). For small $\mathbf{h}_i(s)$, the lowest order nonzero term arises from the term $-(\Delta F_i/4)$ in p_i , giving

$$\left\langle \sum_{i=1}^{Z\bar{v}\Delta t} \mathbf{h}_i(s) y_i \right\rangle = \frac{3h^2 \bar{v}}{4a^2} \Delta t \int \psi(s-s') \left[\frac{\partial^2 \mathbf{r}}{\partial s'^2} - \frac{1}{4} \frac{\partial^4 \mathbf{r}}{\partial s'^4} \right] ds'$$

The remaining noise term $\mathbf{g}(s, t) \Delta t$ is thus dominated by the leading order term $p_i \approx 1/2$ so that its second moment average over the same three quantities is

$$\langle g_{\alpha}(s, t) g_{\beta}(s', t) \rangle = \frac{h^2 \bar{v}}{2\Delta t} \psi(s-s') \delta_{\alpha\beta}$$

Hop attempts between different intervals in time are not correlated, so

$$\langle g_{\alpha}(s, t) g_{\beta}(s', t') \rangle = \frac{h^2 \bar{v}}{2} \psi(s-s') \delta_{\alpha\beta} \frac{\delta_{t,t'}}{\Delta t}$$

Hence, taking the limit $\Delta t \rightarrow 0$ yields the Langevin equation (19).

Appendix D. Envelope Function for Tube Hops

From eq 4 we have a relationship between the centers of the localizing potentials and the mean path, which in the continuum limit is

$$\mathbf{R}(s) = \mathbf{r}(s) - \frac{1}{4} \frac{\partial^2 \mathbf{r}}{\partial s^2}$$

If we envisage a constraint release “hop” as being equivalent to changing the position of one of the localizing potentials at $s = s_m$, we have (again, in the continuum limit)

$$\Delta \mathbf{R}(s) = \mathbf{H} \delta(s - s_m)$$

so that the change $\Delta \hat{\mathbf{r}}$ in mean path obeys

$$\mathbf{H} \delta(s - s_m) = \Delta \hat{\mathbf{r}}(s) - \frac{1}{4} \frac{\partial^2 \Delta \hat{\mathbf{r}}}{\partial s^2}$$

Making use of eq 38, we see that the solution to this is

$$\Delta \hat{\mathbf{r}}(s) = \mathbf{H} \exp(-2|s - s_m|)$$

giving eq 21.

Appendix E. Boundary Conditions

Here, we first consider boundary conditions for a finite chain localized by harmonic potentials (to give what one might call the “real” boundary conditions on the mean path $\hat{\mathbf{r}}$). We then show that the influence of these boundary conditions is short-ranged, suggesting that variations in the boundary conditions can be considered. Finally, we propose two possible alternative boundary conditions which are more tractable within the framework of Graham et al.¹²

When deriving the free energy (6) in the main body of the paper, we did not give explicit considerations to the boundaries. If one performs the same calculation for harmonic potentials attached to a finite Gaussian chain of $N + 1$ beads ($0 \leq l \leq N$) and similarly calculates the effective free energy for the mean path, one obtains

$$F = \frac{1}{2} \sum_{l=0}^{N-1} \frac{3}{b^2} \left(\frac{\partial \hat{\mathbf{r}}}{\partial l} \right)^2 + \frac{1}{2} \sum_{l=1}^{N-1} \frac{3N_s}{b^2} \left(\frac{\partial^2 \hat{\mathbf{r}}}{\partial l^2} \right)^2 + \frac{3N_s}{2b^2} [(\hat{\mathbf{r}}(0) - \hat{\mathbf{r}}(1))^2 + (\hat{\mathbf{r}}(N) - \hat{\mathbf{r}}(N-1))^2] \quad (39)$$

The effective boundary conditions in the continuum limit for such a mean path can be obtained by examining the expression for the “force” $f_\alpha(l) = -\partial F / \partial \hat{r}_\alpha(l)$ near in the center and at the ends of the mean path. We find, for general l ,

$$\mathbf{f}(l) = \frac{3}{b^2} \left(\frac{\partial^2 \hat{\mathbf{r}}}{\partial l^2} - N_s \frac{\partial^4 \hat{\mathbf{r}}}{\partial l^4} \right)$$

while for $l = 0$ and $l = 1$

$$\begin{aligned} \mathbf{f}(0) &= \frac{3}{b^2} (\hat{\mathbf{r}}(1) - \hat{\mathbf{r}}(0)) - \frac{3N_s}{b^2} (\hat{\mathbf{r}}(2) - 3\hat{\mathbf{r}}(1) + 2\hat{\mathbf{r}}(0)) \\ \mathbf{f}(1) &= \frac{3}{b^2} (\hat{\mathbf{r}}(2) + \hat{\mathbf{r}}(0) - 2\hat{\mathbf{r}}(1)) - \frac{3N_s}{b^2} (\hat{\mathbf{r}}(3) - 4\hat{\mathbf{r}}(2) + 6\hat{\mathbf{r}}(1) - 3\hat{\mathbf{r}}(0)) \end{aligned}$$

The equations for $\mathbf{f}(0)$ and $\mathbf{f}(1)$ can be made equivalent to that for $\mathbf{f}(l)$ if we define virtual “boundary beads” at $\hat{\mathbf{r}}(-1)$ and $\hat{\mathbf{r}}(-2)$ such that

$$\begin{aligned} \hat{\mathbf{r}}(-1) &= \hat{\mathbf{r}}(0) \\ \hat{\mathbf{r}}(-2) &= \hat{\mathbf{r}}(1) \end{aligned}$$

which suggests continuum boundary conditions of

$$\frac{\partial \hat{\mathbf{r}}}{\partial s} = \frac{\partial^3 \hat{\mathbf{r}}}{\partial s^3} = \mathbf{0} \quad (40)$$

at the chain ends.

In the continuous description of the tube, we can investigate how far along the path these boundary conditions have an effect on the equilibrium conformations of $\hat{\mathbf{r}}(s)$. They suggest that we can write a Fourier expansion of $\hat{\mathbf{r}}(s)$ for $0 \leq s \leq Z$ as

$$\hat{\mathbf{r}}(s) = \mathbf{X}_0 + \sum_p \mathbf{X}_p \cos\left(\frac{p\pi s}{Z}\right)$$

and substituting into (7) with $\kappa = 1/4$ gives

$$F = \frac{1}{2} \sum_p \frac{6\pi^2 p^2}{a^2 Z} \left(1 + \frac{\pi^2 p^2}{4Z^2} \right) \mathbf{X}_p^2$$

so that, in equilibrium,

$$\langle X_{\alpha,p} X_{\beta,p'} \rangle = \frac{a^2 Z}{6\pi^2 p^2} \left(1 + \frac{\pi^2 p^2}{4Z^2} \right)^{-1} \delta_{pp'} \delta_{\alpha\beta}$$

and so

$$\left\langle \frac{\partial \hat{r}_\alpha}{\partial s} \frac{\partial \hat{r}_\beta}{\partial s} \right\rangle = \frac{2a^2}{3Z} \delta_{\alpha\beta} \sum_p \left(1 + \frac{\pi^2 p^2}{4Z^2} \right)^{-1} \sin^2\left(\frac{p\pi s}{Z}\right)$$

Near $s = 0$ and for large Z we can replace the sum by an integral ($\sum_p \rightarrow \int_0^\infty dp$) and make the substitution $q = p\pi/Z$, giving

$$\begin{aligned} \left\langle \frac{\partial \hat{r}_\alpha}{\partial s} \frac{\partial \hat{r}_\beta}{\partial s} \right\rangle &= \frac{2a^2}{3\pi^2} \delta_{\alpha\beta} \int_0^\infty dq \left(1 + \frac{q^2}{4} \right)^{-1} \sin^2(qs) \\ &= \frac{a^2}{3} \delta_{\alpha\beta} (1 - \exp(-4s)) \end{aligned}$$

This expression indicates that the effect of the boundary conditions is very short range and is confined within a region of, at most, one tube diameter from the chain ends. Hence, the precise choice of boundary conditions cannot be very significant for the main portion of a well-entangled chain. Furthermore, under most flow conditions, the tube ends are rapidly moving compared to flow time scales and thus attain their equilibrium configuration subject to the influence of boundary conditions and the “inner” tube sections.

Unfortunately, the boundary conditions of eq 40 cause problems when used within the theory of Graham et al.,¹² specifically when applied to the reptation and retraction terms (which we have taken directly from their theory). Quantities such as the tube tangent and the local stretch, which are constructed with the inner tube sections in mind, are not defined at the boundaries given by eq 40. We consider that resolution of this latter issue is not possible without addressing the transition between 1D motion along the tube and 3D motion at the chain ends, and also addressing the stochastic noise for along-tube motion, beyond the noise for the reptation mode. Such considerations, though interesting, are likely to cause only small changes near the boundaries and so are very unlikely to affect the main conclusions of this work.

For these reasons, we have investigated two possible pragmatic choices of boundary condition for the constitutive equation set given in Appendix D, one in which $f_{\alpha\beta}(s, s')$ is set equal to its equilibrium $f_{\alpha\beta}^{\text{eq}}(s, s')$ outside the range $0 \leq s \leq Z$ and $0 \leq s' \leq Z$, and a second which corresponds to a long, but equilibrated, section of tube attached at the chain end. The latter choice is motivated by the suggestion that there is very little difference between this and a short but similarly equilibrated tube end with boundary conditions as given above: the fluctuations in the forces experienced by the central portion of the chain will be identical in both cases. In practice, however, we find that either choice of boundary condition gives very similar results and note further that the first choice is somewhat easier to implement.

References and Notes

- (1) McLeish, T. C. B. *Adv. Phys.* **2002**, *51*, 1379–1527.
- (2) Doi, M.; Edwards, S. F. *The Theory of Polymer Dynamics*; Clarendon: Oxford, 1986.
- (3) Likhtman, A. E. *Macromolecules* **2005**, *38*, 6128–6139.
- (4) Schieber, J. D.; Nair, D. M.; Kitkrailard, T. J. *Rheol.* **2007**, *51*, 1111–1141.
- (5) Doi, M.; Takimoto, J. *Philos. Trans. R. Soc. London A* **2003**, *361*, 641–650.
- (6) Masubuchi, Y.; Ianniruberto, G.; Greco, F.; Marrucci, G. *Modell. Simul. Mater. Sci. Eng.* **2004**, *12*, S91–S100.

- (7) Marrucci, G. *J. Non-Newtonian Fluid Mech.* **1996**, *62*, 279–289.
- (8) Tapiada, P.; Wang, S. Q. *Macromolecules* **2004**, *24*, 9083–9095.
- (9) Ianniruberto, G.; Marrucci, G. *J. Rheol.* **2001**, *45*, 1305–1318.
- (10) Mead, D. W.; Larson, R. G.; Doi, M. *Macromolecules* **1998**, *31*, 7895–7914.
- (11) Pattamaprom, C.; Driscoll, J. J.; Larson, R. G. *Macromol. Symp.* **2000**, *158*, 1–13.
- (12) Graham, R. S.; Likhtman, A. E.; McLeish, T. C. B.; Milner, S. T. *J. Rheol.* **2003**, *47*, 1171–1200.
- (13) Read, D. J. *J. Rheol.* **2004**, *48*, 349–377.
- (14) de Gennes, P. G. *J. Phys. (Paris)* **1981**, *42*, 735.
- (15) Likhtman, A. E.; Sukumaran, S. K.; Ramirez, J. *Macromolecules* **2007**, *40*, 6748–6757.
- (16) Warner, M.; Edwards, S. F. *J. Phys. A* **1978**, *11*, 1649–1655.
- (17) Read, D. J.; McLeish, T. C. B. *Macromolecules* **1997**, *30*, 6376–6384.
- (18) Mergell, B.; Everaers, R. *Macromolecules* **2001**, *34*, 5675–5686.
- (19) Deam, R. T.; Edwards, S. F. *Philos. Trans. R. Soc. London A* **1976**, *280*, 317.
- (20) Ramirez, J.; Sukumaran, S. K.; Likhtman, A. E. *J. Chem. Phys.* **2007**, *126*, 244904.
- (21) Viovy, J. L.; Rubinstein, M.; Colby, R. H. *Macromolecules* **1991**, *24*, 3587–3596.
- (22) Rubinstein, M.; Panyukov, S. *Macromolecules* **1997**, *30*, 8036–8044.
- (23) Rubinstein, M.; Panyukov, S. *Macromolecules* **2002**, *35*, 6670–6686.

MA8009855